

Neutralizing activity of Sputnik V vaccine sera against SARS-CoV-2 variants

Satoshi Ikegame

Icahn School of Medicine at Mount Sinai <https://orcid.org/0000-0002-8183-3527>

Mohammed Siddiquey

Louisiana State University Health Shreveport

Chuan-Tien Hung

Icahn School of Medicine at Mount Sinai

Griffin Haas

Icahn School of Medicine at Mount Sinai

Luca Brambilla

Icahn School of Medicine at Mount Sinai,

Kasopefoluwa Oguntuyo

Icahn School of Medicine

Sheryas Kowdle

Icahn School of Medicine at Mount Sinai

Ariel Vilardo

National Administration of Laboratories and Health Institutes of Argentina (ANLIS) Dr. Carlos G. Malbran

Alexis Edelstein

National Administration of Laboratories and Health Institutes of Argentina (ANLIS) Dr. Carlos G. Malbran

Claudia Perandones

National Administration of Laboratories and Health Institutes of Argentina (ANLIS) Dr. Carlos G. Malbran

Jeremy Kamil

Louisiana State University Health Science Center Shreveport <https://orcid.org/0000-0001-8422-7656>

Benhur Lee (✉ benhur.lee@mssm.edu)

Icahn School of Medicine at Mount Sinai <https://orcid.org/0000-0003-0760-1709>

Biological Sciences - Article

Keywords: SARS-CoV-2, vaccine development, variants

Posted Date: April 8th, 2021

DOI: <https://doi.org/10.21203/rs.3.rs-400230/v1>

License:  This work is licensed under a Creative Commons Attribution 4.0 International License.

[Read Full License](#)

Version of Record: A version of this preprint was published at Nature Communications on July 26th, 2021. See the published version at <https://doi.org/10.1038/s41467-021-24909-9>.

1 **Neutralizing activity of Sputnik V vaccine sera against SARS-CoV-2 variants**

2

3 Satoshi Ikegame^{1,#}, Mohammed N. A. Siddiquey^{2,#}, Chuan-Tien Hung¹, Griffin Haas¹,
4 Luca Brambilla¹, Kasopefoluwa Y. Oguntuyo¹, Shreyas Kowdle¹, Ariel Esteban Vilardo³,
5 Alexis Edelstein³, Claudia Perandones^{3,†}, Jeremy P. Kamil^{2,†}, and Benhur Lee^{1,†,*}

6

7 **Affiliations.**

8 1. Department of Microbiology at the Icahn School of Medicine at Mount Sinai, New
9 York, NY 10029, USA

10 2. Department of Microbiology and Immunology, Louisiana State University Health
11 Shreveport, Shreveport, LA 71103, USA.

12 3. National Administration of Laboratories and Health Institutes of Argentina (ANLIS) Dr.
13 Carlos G. Malbrán, Buenos Aires, Argentina

14 # These authors contributed equally to the study.

15 † Senior authors

16 * Correspondence to: Benhur Lee, benhur.lee@mssm.edu

17

18 **Competing interests:** B.L. and K.Y.O. are named inventors on a patent filed by the
19 Icahn School of Medicine for some of the materials used in this work. J.P.K. is a
20 consultant for BioNTech (advisory panel on coronavirus variants).

21

22

23

24 **ABSTRACT.**

25 The novel pandemic betacoronavirus, severe acute respiratory syndrome coronavirus 2
26 (SARS-CoV-2), has infected at least 120 million people since its identification as the
27 cause of a December 2019 viral pneumonia outbreak in Wuhan, China^{1,2}. Despite the
28 unprecedented pace of vaccine development, with six vaccines already in use
29 worldwide, the emergence of SARS-CoV-2 ‘variants of concern’ (VOC) across diverse
30 geographic locales have prompted re-evaluation of strategies to achieve universal
31 vaccination³. All three officially designated VOC carry Spike (S) polymorphisms thought
32 to enable escape from neutralizing antibodies elicited during initial waves of the
33 pandemic⁴⁻⁸. Here, we characterize the biological consequences of the ensemble of S
34 mutations present in VOC lineages B.1.1.7 (501Y.V1) and B.1.351 (501Y.V2). Using a
35 replication-competent EGFP-reporter vesicular stomatitis virus (VSV) system, rcVSV-
36 CoV2-S, which encodes S from SARS coronavirus 2 in place of VSV-G, and coupled
37 with a clonal HEK-293T ACE2 TMPRSS2 cell line optimized for highly efficient S-
38 mediated infection, we determined that only 1 out of 12 serum samples from a cohort of
39 recipients of the Gamaleya Sputnik V Ad26 / Ad5 vaccine showed effective
40 neutralization (IC₉₀) of rcVSV-CoV2-S: B.1.351 at full serum strength. The same set of
41 sera efficiently neutralized S from B.1.1.7 and showed only moderately reduced activity
42 against S carrying the E484K substitution alone. Taken together, our data suggest that
43 control of some emergent SARS-CoV-2 variants may benefit from updated vaccines.

44

45 SARS-CoV-2 is closely related to two other zoonotic betacoronaviruses, MERS-CoV
46 and SARS-CoV, that also cause life-threatening respiratory infections⁹. The global
47 health emergency caused by the spread of SARS-CoV-2 has spurred the development
48 of COVID-19 preventive vaccines at an unprecedented pace. Six are already authorized
49 for human use across the globe^{10–15}. These vaccines focus on the SARS-CoV-2 spike
50 protein (S), due to its critical roles in cell entry. Indeed, the presence of serum
51 neutralizing antibodies directed at S correlate strongly with protection against COVID-19
52^{16,17}. Although these six vaccines are efficacious, the recent emergence of novel SARS-
53 CoV-2 variants has reignited concerns that the pandemic may not be so easily brought
54 under control.

55 In December 2020, the United Kingdom reported the sudden emergence of a novel
56 SARS-CoV-2 lineage, termed B.1.1.7 (501Y.V1, VOC 202012/01), which was
57 designated as the first SARS-CoV-2 variant of concern (VOC). The lineage had rapidly
58 increased in prevalence since first being detected in November 2020¹⁸. Its genome
59 showed an unusually high number of non-synonymous substitutions and deletions,
60 including eight in the S gene, suggesting a substantial degree of host adaptation that
61 may have occurred during prolonged infection of an immunocompromised person¹⁹.
62 The B.1.1.7 lineage has now been shown to exhibit enhanced transmissibility²⁰ as well
63 as an increased case fatality rate^{21,22}.

64 Soon afterwards, two additional SARS-CoV-2 VOC, B.1.351 and P.1, were
65 reported from S. Africa and Brazil, respectively, which each showed substantial escape
66 from neutralizing antibodies elicited by first wave pandemic viruses, leading to
67 documented cases of re-infection^{23–25}. The S genes of B.1.351 and P.1 viruses each
68 carry a number of mutations, but include three in the receptor binding domain (RBD)
69 that are particularly notable, the S: N501Y substitution, found in B.1.1.7, alongside
70 polymorphisms at positions 417 and 484, K417N/T and E484K. S: E484K had already
71 been identified in multiple independent laboratories to confer escape from convalescent
72 sera and monoclonal antibodies^{26–28}. As expected, the P.1 and B.1.351 variants escape
73 or resist neutralization by first wave convalescent sera, as well as antibodies elicited by
74 COVID-19 vaccines^{4–8}.

75 Although the P.1 and B.1.351 lineages are dominant in Brazil and S. Africa,
76 unlike B.1.1.7 they have not increased greatly in number in the United States since
77 originally being detected here. In contrast, the E484K polymorphism is recurrently
78 emergent, and is found in a number of other lineages that are increasing in the U.S. and
79 other countries. For example, a B.1.526 sub-lineage carrying E484K in recent weeks
80 has expanded more rapidly than B.1.1.7^{29,30}, which may be indicative of the ability of S:
81 E484K variants to penetrate herd immunity. The P.2 lineage, originally detected in Rio
82 de Janeiro, carries only the E484K mutation in the RBD and has spread to other parts of
83 South America, including Argentina³¹.

84 The six COVID-19 vaccines currently in use around the world employ different
85 strategies, and do not all incorporate the two proline substitutions that “lock” S into the

86 pre-fusion conformer. Vaccines that do not utilize pre-fusion “locked” S are expected to
87 produce lower levels of neutralizing antibodies, and hence may be less efficacious
88 against infection, even if they do protect against severe COVID-19. Indeed, a two-dose
89 regimen of the AstraZeneca ChAdOx1 based vaccine, which does not use a “locked” S,
90 did not protect against mild-to-moderate COVID-19 in S. Africa, where 93% of COVID-
91 19 cases in trial participants were caused by the B.1.351 variant ³². Like the
92 AstraZeneca ChAdOx1 vaccine, the Sputnik V vaccine (Gam-COVID-Vac) is based on
93 adenovirus vectored expression of a native S sequence, rather than a pre-fusion
94 “locked” S ³³. Although the Sputnik V vaccine has a reported vaccine efficacy of 91.6%
95 in the interim analysis of Phase 3 trials held in Russia between Sept 7 and Nov 24,
96 2020, none of the VOC mentioned above nor independent lineages containing the
97 E484K mutation were prevalent in Russia during this time period. Since the Sputnik
98 vaccine is now in use not only in Russia, but also in countries like Argentina, Mexico,
99 and Hungary, where some of the VOC and emerging lineages bearing the E484K
100 mutation are more widespread, it is critical to assess the neutralizing activity of Sputnik
101 vaccine elicited antibody responses against these cognate VOC and mutant spikes.

102 This study characterizes the neutralization activity of sera from a dozen Sputnik
103 V vaccine recipients in Argentina. Our work was spurred by Argentina’s nascent
104 genomic surveillance efforts, which detected multiple independent lineages with S:
105 E484K (B.1.1.318 and P.2) and/or S: N501Y substitutions (B.1.1.7 and P.1) in common,
106 just as Argentina had started rolling out its vaccination campaign, which commenced on
107 Dec 29, 2020. Here, we generated isogenic replication-competent vesicular stomatitis
108 virus bearing the prevailing wild-type (WT=D614G) SARS-CoV-2 S (rcVSV-CoV2-S), or
109 the B.1.1.7, B.1.351 or E484K mutant S and used them in a robust virus neutralization
110 assay. Our results show that Sputnik V vaccine sera effectively neutralized S: WT and
111 S: B.1.1.7. viruses, albeit with highly variable titers. The same sera, however, exhibited
112 moderate and markedly reduced neutralization titers, respectively, against S: E484K
113 and S: B.1.351. Analyses of dose response curves indicate that S: B.1.351 exhibits
114 resistance to neutralizing sera in a manner that is qualitatively different from the E484K
115 mutant. Taken together, our data argue that surveillance of the neutralizing activity
116 elicited by vaccine sera will be necessary on an ongoing basis. Viral neutralization
117 assays can indicate which SARS-CoV-2 variants are likely capable of transmission in
118 the face of vaccine elicited immunity, and whether updated vaccines will be needed to
119 control their emergence and spread.

120

121 **RESULTS.**

122 **Robust reverse genetics for generating replication-competent VSV expressing**
123 **SARS-CoV-2 Spike proteins.**

124 Several groups have now generated replication-competent VSV expressing SARS-CoV-
125 2 spike in place of VSV-G (rcVSV-CoV2-S)^{34–36,37}. These rcVSV-CoV2-S can be used in
126 BSL-2 compatible virus neutralization assays (VNAs), which correlate very well with
127 VNAs using live SARS-CoV-2 (Spearman's $r > 0.9$ across multiple studies). rcVSV-
128 CoV2-S has been assessed as a candidate vaccine^{36,38}, and used in forward genetics
129 experiments to generate antibody escape mutants or perform comprehensive epitope
130 mapping studies^{39,26,37}. Indeed, the now concerning E484K mutation, present in many
131 variants of concern (VOC), was identified as an antibody escape mutation using rcVSV-
132 CoV-2-S^{26,37}.

133 However, many groups passage their rcVSV-CoV-2-S extensively in Vero cells after the
134 initial rescue, either to generate higher titer stocks and/or to remove confounding
135 components such as the vaccinia virus expressing T7-polymerase and/or transfected
136 VSV-G, both of which were deemed necessary for efficient rescue³⁷. Serial passage of
137 rcVSV-CoV-2-S in Vero cells invariably leads to mutations in the S1/S2 furin cleavage
138 site, as well as truncations in the cytoplasmic tail of the S protein³⁸. The latter promotes
139 S incorporation into VSV without compromising the conformational integrity of the
140 ectodomain, whereas the former is problematic when assessing the neutralization
141 sensitivity and structure-function phenotype of Spike VOC with multiple mutations that
142 likely have complex epistatic interactions.

143 To generate rcVSV-CoV2-S containing different variants or mutants on demand, without
144 the need for extensive passaging, we developed a robust reverse genetics system and
145 VNA which leverages the cell lines we previously developed for a standardized SARS-
146 CoV-2 VNA that correlates well with live virus neutralization⁴⁰. Salient improvements
147 include the addition of a hammerhead ribozyme immediately upstream of the 3' leader
148 sequence which cleaves *in cis* to give the exact 3' termini, the use of a codon-optimized
149 T7-polymerase which alleviates the use of vaccinia-driven T7-polymerase, and a highly
150 permissive and transfectable 293T-ACE2+TMPRSS2 clone (F8-2)⁴⁰ (Extended Data
151 Fig S1). A 6-plasmid transfection into F8-2 cells results in GFP+ cells 2-3 days post-
152 transfection (dpt), which turn into foci of syncytia by 4-5 dpt indicating virus replication
153 and cell-to-cell spread (Fig. 1A). Transfer of F8-2 cell supernatant into interferon-
154 defective Vero-TMPRSS2 cells allowed for rapid expansion of low-passage viral stocks
155 that maintain only the engineered Spike mutations. Clarified viral supernatants from
156 Vero-TMPRSS2 cells were aliquoted, sequenced verified, then titered on F8-2 cells to
157 determine the linear range of response (Fig. 1B).

158 Next, we generated isogenic rcVSV-CoV2-S expressing the B.1.1.7, B.1.351 (Fig. 2A),
159 or E484K S to evaluate the neutralizing activity of Sputnik V vaccine sera from
160 Argentina. The relevant Spike substitutions that make up these variants are indicated in

161 Fig. 2A. The characteristics of the vaccine recipient cohort (n=12) receiving the two-
162 dose regimen of the Sputnik vaccine are given in Table 1. At one month post-
163 completion of the two-dose regimen, the Sputnik V vaccine generated respectable virus
164 neutralizing titers (VNT) against rcVSV-CoV2-S bearing the WT (D614G) and B.1.1.7
165 spike proteins (Fig. 2B). The geometric mean titer (GMT) and 95% CI for WT (1/IC₅₀
166 GMT 49.4, 23.4 - 105) in our cohort of vaccine recipients was remarkably similar to that
167 reported in the phase III Sputnik vaccine trial (GMT 44.5, 31.8 - 62.2)¹⁰. However, GMT
168 against B.1.351 and E484K was reduced by a median 6.8- and 2.8-fold, respectively
169 compared to WT (Fig. 2C).

170 Sputnik vaccine recipients appeared to generate qualitatively different neutralizing
171 antibody responses against SARS-CoV-2 (Fig.3A-D and Extended Data Fig. S2) that
172 segregated into 4 different groups. Group (A) exemplified by SP009 showed
173 reasonable VNT against wild-type (WT) and B.1.1.7 (reciprocal IC₅₀ = 76 and 111,
174 respectively, Fig. 3A and E). However, the Hill slope of the neutralization curve for
175 B.1.351 was extremely shallow (h=0.39). This class of sera achieves a maximal
176 neutralization of 50-60% even when extrapolated to full serum strength (1/serum dilution
177 = 1). In contrast, although the reciprocal IC₅₀ for E484K is moderately decreased (VNT
178 = 23), it is clear that E484K will still be neutralized at higher serum concentrations due
179 to a significantly steeper Hill slope (h=1.4). Group (B) sera generally exhibit effective
180 neutralization of WT, B.1.1.7, and even E484K at high serum concentrations, but not
181 B.1.351 (Fig. 3B and E). The decreased potency and shallow Hill Slope result in <90%
182 neutralization of B.1.351 even at full serum strength. Group (C) sera neutralize E484K
183 and B.351 with potencies similar to WT and B.1.1.7, especially at high serum
184 concentrations (Fig. 3C and E). This group of sera reveals that qualitatively different
185 neutralizing responses can be generated that can effectively neutralize B.1.351. The
186 one serum in Group (D) appears unique. It exhibited little to no neutralizing activity
187 against WT, E484K and B.1.351, yet it neutralized B.1.1.7 as well as Group A-C sera.
188 This is obvious when comparing the reciprocal IC₅₀s for B.1.1.7 (blue squares) across
189 the four different groups of sera in Fig.3D and E).

190 The heterogenous dose-response curves described in Fig. 3 (and Extended Data Fig.
191 S2) is a property of Sputnik V vaccine elicited responses as soluble RBD-Fc inhibition of
192 WT and VOC S-mediated entry produced classical dose response curves with Hill
193 slopes close to -1.0 (Fig. 4A). Both B.1.1.7 and B.1.351 were modestly but significantly
194 more resistant to RBD-Fc inhibition (Fig. 4B). This is not surprising as both harbor the
195 N501Y mutation known to enhance affinity of RBD for ACE2. However, this 1.5 to 2-fold
196 increase in RBD-Fc IC₅₀ for B.1.1.7 and B.1.351, respectively, does not explain the
197 neutralization-resistant versus sensitive phenotype of B.1.351 versus B.1.1.7 in our
198 virus neutralization assays. Interestingly, each VOC or mutant clustered differently in
199 the neutralization phenotype landscape defined by both IC₅₀ and slope (Fig. 4C).

200 These data suggest that the cognate VOC exhibit qualitatively distinct modes of escape
201 from Sputnik vaccine neutralization ⁴¹.

202

203

204 **DISCUSSION**

205 A key public health concern related to emergent SARS-CoV-2 variants is that by
206 incrementally accruing mutations that escape neutralizing antibodies, they will penetrate
207 herd immunity and spread to reach unvaccinated individuals, some of whom will be
208 susceptible to severe or fatal disease.

209 Three of the six COVID-19 vaccines currently in use worldwide, namely Moderna
210 mRNA-1273, BioNTech BNT162b2, and Janssen Ad26.COV2.S, each express S
211 harboring K986P and V987P substitutions (2P) within a loop abutting the central helix of
212 the S2' membrane fusion machinery⁴²⁻⁴⁴. This modification locks the spike in a
213 prefusion conformation and elicits higher titers of neutralizing antibodies^{45,46}. Of the
214 three vaccines that do not appear to make use of 2P Spike mutants, Gamaleya's
215 Sputnik V and AstraZeneca's AZD1222 are adenovirus-vectored vaccines encoding
216 native S. The third is CoronaVac, a preparation of inactivated SARS-CoV-2 virions.
217 Although all six vaccines are highly efficacious at preventing severe COVID-19
218 outcomes, they do not all uniformly prevent infection. Moreover, in all cases thus far
219 examined, these first generation vaccines are less effective against variants with certain
220 non-synonymous substitutions in Spike, such as E484K.

221 The most concerning variants are those with multiple mutations in the receptor binding
222 domain (RBD) that confer both enhanced affinity for the hACE2 receptor and escape
223 from neutralizing antibody responses^{5,8,23,32,47,48}. B.1.351 and P.1 have in common
224 three RBD substitutions (K417N/T, E484K and N501Y) whereas all three WHO
225 designated VOC contain the N501Y substitution. Although B.1.1.7 shows enhanced
226 transmissibility and more severe disease outcomes^{20,21}, it does not appear to be
227 consistently more resistant to serum neutralizing responses elicited by vaccines or
228 natural infection^{49,50}. The same is not true, however, for the B.1.351 variant.

229 In live virus plaque reduction neutralization assays, sera from AstraZeneca vaccine
230 recipients in South Africa exhibited 4.1 to 32.5-fold reduction in neutralizing activity
231 against B.1.351³². The actual reduction is even more marked because 7 of 12 vaccine
232 recipients who had neutralizing activity against the parental B.1.1 variant, had
233 undetectable neutralization against the B.1.351 strain. Comparator sera from recipients
234 of Moderna and BioNTech mRNA vaccines showed smaller, 6.5 to 8.6-fold reductions in
235 neutralization⁵¹.

236 As of this writing, there is no data on the protective efficacy of Sputnik V and CoronaVac
237 against SARS-CoV-2 S variants. Here, we showed that sera from Sputnik vaccine
238 recipients in Argentina had a median 6.1-fold and 2.8-fold reduction in GMT against
239 B.1.351 and the E484K mutant spike, respectively. Even more revealing is their dose-
240 response curves. When extrapolated to full serum strength, half of the sera samples
241 failed to achieve an IC₈₀ and only 1 out 12 achieved an IC₉₀. (Extended Data Fig. S3).
242 One serum had little to no detectable neutralizing activity against B.1.351, E484K and
243 even WT, but neutralized B.1.1.7 effectively. Altogether, these data suggest vaccines

244 that do not use the 2P stabilized Spike appear to generate more variable neutralizing
245 responses that make it difficult to establish immune correlates of protection, especially
246 against emerging VOC/VOI that contain the recurrent E484K mutation.

247 E484K is present not only as part of an ensemble of RBD mutations present in B.1.351
248 and P.1, but in many of the 17 lineages detected from South America that carry it, such
249 as P.2, E484K is the only RBD substitution (Supplementary Table 1). A more detailed
250 report covering the genomic surveillance efforts in Argentina that detected the VOC
251 which spurred our study is currently in preparation (Dr. Claudia Perandones, personal
252 communication).

253 While the E484K substitution appears to be a common route of escape from many
254 RBD-targeting monoclonal antibodies, it is somewhat surprising that a single mutation
255 can confer a significant degree of neutralization resistance from polyclonal responses.
256 Nonetheless, our data show that resistance conferred by E484K mutation be overcome
257 by higher titer antibodies present in undiluted patient sera. But the neutralization
258 resistance conferred by the suite of mutations present in B.1.351 appears qualitatively
259 different. In the majority of cases, the slope of the dose response curve indicates a
260 failure to neutralize even at full strength. We had previously shown that the dose-
261 response curve slope is a major predictor of therapeutic potency for HIV broadly
262 neutralizing antibodies at clinically relevant concentrations ⁴¹. Importantly, the slope
263 parameter is independent of IC50 but is specifically related to an antibody's epitope
264 class. Here, we show that defining the neutralization phenotype of a given spike variant
265 or mutant by both its relative IC50 and slope provides a fuller characterization of serum
266 neutralizing activity against SARS-CoV-2 spike and the emergent VOC.

267 Although we stress that the Gamelya Sputnik V vaccine is likely to retain strong efficacy
268 at preventing severe COVID-19, even in the case of infection by VOC, our data reveal a
269 concerning potential of B.1.351, and to a lesser extent, any variant carrying the E484K
270 substitution (e.g. P.2), to escape the neutralizing antibody responses that this
271 immunization elicits. Furthermore, we acknowledge that *in vivo* protective efficacy can
272 be derived from Fc effector functions of antibodies that bind but do not neutralize. In
273 addition, an adenoviral vectored vaccine should induce potent cell-mediated immunity
274 against multiple epitopes, which were not measured in our study. Nevertheless, given
275 the crucial roles neutralizing antibodies play in preventing infection, our results suggest
276 that updated SARS-CoV-2 vaccines will be necessary to eliminate the virus.

277

278 **Materials and Methods**

279

280 **Cell lines**

281 Vero-CCL81 TMPRSS2, HEK 293T-hACE2 (clone 5-7), and 293T-hACE2-TMPRSS2
282 (clone F8-2) cells were described previously ⁴⁰, and were maintained in DMEM +

283 10%FBS. The HEK 293T-hACE2-TMPRSS2 cells were plated on collagen coated
284 plates or dishes. BSR-T7 cells⁵², which stably express T7-polymerase were maintained
285 in DMEM with 10% FBS.

286 **VSV-eGFP-CoV2 spike (Δ 21aa) genomic clone and helper plasmids.**

287 We cloned VSV-eGFP sequence into pEMC vector (pEMC-VSV-eGFP), which includes
288 an optimized T7 promoter and hammerhead ribozyme just before the 5' end of the viral
289 genome. The original VSV-eGFP sequence was from pVSV-eGFP, a generous gift of
290 Dr. John Rose⁵³.

291 We generated pEMC-VSV-eGFP-CoV2-S (Genbank Accession: MW816496) as follows:
292 the VSV-G open reading frame of pEMC-VSV-eGFP was replaced with the SARS-CoV-
293 2 S, truncated to lack the final 21 amino acids⁵⁴. We introduced a Pac-I restriction
294 enzyme site just after the open reading frame of S transcriptional unit, such that the S
295 transcriptional unit is flanked by MluI / PacI sites. SARS-CoV-2 S is from pCAGGS-
296 CoV-2-S⁵⁵, which codes the codon optimized S from the Wuhan Hu-1 isolate (NCBI ref.
297 seq. NC_045512.2) with a point mutation of D614G, resulting in B.1 lineage. The
298 B.1.1.7 Spike we used carries the mutations found in GISAID Accession Number
299 EPI_ISL_668152: del 69-70, del145, N501Y, A570D, D614G, P681H, T716I, S982A,
300 and D1118H. The B.1.351 Spike carries the mutations D80A, D215G, del242-244,
301 K417N, E484K, N501Y, D614G, and A701V (from EPI_ISL_745109). The Spike
302 sequences of WT, B.1.1.7, B.1.351, and E484K are available at Genbank (Accession
303 Numbers: MW816497, MW816498, MW816499, and MW816500; please also see
304 Supplemental Table 2).

305 Sequences encoding the VSV N, P, M, G, and L proteins were also cloned into pCI
306 vector to make expression plasmids for virus rescue, resulting in plasmids: pCI-VSV-N,
307 pCI-VSV-P, pCI-VSV-M, pCI-VSV-G, and pCI-VSV-L. These accessory plasmids were a
308 kind gift from Dr. Benjamin tenOever.

309 **Generation of VSV-CoV2 spike from cDNA**

310 4×10^5 293T-ACE2-TMPRSS2 cells per well were seeded onto collagen-I coated 6 well
311 plates. The next day, 2000 ng of pEMC-VSV-EGFP-CoV2 spike, 2500 ng of pCAGGS-
312 T7opt⁵⁶, 850 ng of pCI-VSV-N, 400 ng of pCI-VSV-P, 100 ng of pCI-VSV-M, 100 ng of
313 pCI-VSV-G, 100 ng of pCI-VSV-L were mixed with 4 mL of Plus reagent and 6.6 mL of
314 Lipofectamine LTX (Invitrogen). 30 min later, transfection mixture was applied to 293T-
315 hACE2-TMPRSS2 cells in a dropwise fashion. Cells were maintained with medium
316 replacement every day for 4 to 5 days until GFP positive syncytia appeared. Rescued
317 viruses were amplified in Vero-CCL81 TMPRSS2 cells⁴⁰, then titered and used for the
318 assay.

319

320 **Virus neutralization assay**

321 5 x 10⁴ 293T-hACE2-TMPRSS2 cells per well were seeded onto collagen-coated 96
322 well cluster plates one day prior to use in viral neutralization assays. Virus stocks were
323 mixed with serially diluted serum for 10 minutes at room temperature, then infected to
324 cells. Note: all sera assayed in this study were previously heat inactivated by 56
325 degrees for 30 min before use in any viral neutralization studies. At 10 h post infection,
326 GFP counts were counted by Celigo imaging cytometer (Nexcelom). Each assay was
327 done in triplicate. For calculation of IC₅₀, GFP counts from “no serum” conditions were
328 set to 100%; GFP counts of each condition (serum treated) were normalized to no
329 serum control well. Inhibition curves were generated using Prism 8.4.3 (GraphPad
330 Software) with ‘log (inhibitor) vs normalized response - variable slope’ settings.

331

332 **Design of RBD-Fc producing Sendai virus**

333 Sendai virus (SeV) Z strain cDNA sequence (AB855655.1) was generated and cloned
334 into pRS vector with the addition of eGFP transcriptional unit at the head of SeV
335 genome. The sequence of F transcriptional unit was from SeV fushimi strain
336 (KY295909.1) due to the cloning reason. We refer to the pRS-based plasmid coding this
337 sequence as pRS-SeVZ-GFP-F^{fushimi} in this paper. For the introduction of foreign gene
338 into SeV, we generated additional transcriptional unit for RBD-Fc between P gene and
339 M gene. RBD-Fc construct was generated as below; codon optimized DNA sequence of
340 from SARS-CoV-2 spike (MN908947) in pCAGGS a gift of Dr. Florian Krammer⁵⁵. S
341 amino acids 319 – 541 (corresponding to the RBD domain) sequence were C-terminally
342 fused to the Fc region of human IgG₁ (220 – 449 aa of P0DOX5.2)

343

344 **Generation of recombinant Sendai virus from cDNA.**

345 2x10⁵ BSR-T7 cells per well were seeded onto 6-well cluster plates. The next day, 4
346 µg of pRS-SeVZ-GFP-F^{fushimi}, 4 µg of pCAGGS-T7opt, 1.44 µg of SeV-N, 0.77 µg of
347 SeV-P, 0.07 µg of SeV-L were mixed with 5.5 µl of Plus reagent and 8.9 µl of
348 Lipofectamine LTX (Invitrogen). 30 min later, transfection mixtures were applied to Bsr-
349 T7 cells in a dropwise fashion, as described previously⁵⁶. At one day post transfection,
350 medium was replaced with DMEM + 0.2 µg/ml of TPCK-trypsin (Millipore Sigma,
351 #T1426), with subsequent medium replacement each day until infection reached 100%
352 cytopathic effect. Supernatants were stored at -80°C until use in experiments.

353

354 **Titration of viruses.**

355 For SeV titration, 2 x 10⁴ Bsr-T7 cells per well were seeded onto 96-well plates. The
356 next day, 100 µL of serially diluted virus stock (in DMEM + 10% FBS) were applied to
357 each well. GFP positive foci were counted at 24 hours post infection using a Celigo

358 imaging cytometer (Nexcelom, Inc.). Infectivity is presented in infectious units (IU) per
359 mL.

360 For VSV-CoV2 titration, 5×10^4 293T-hACE2-TMPRSS2 cells per well were seeded
361 onto a collagen-coated 96 well plate. Serially diluted virus stocks were then applied to
362 the cells, and GFP positivity was scored at 10 h post infection using a Celigo imaging
363 cytometer.

364

365 **Production of proteins and purification.**

366 5×10^6 Bsr-T7 cells are seeded in T175cm²-flask one day before infection. Cells were
367 infected by SeV at MOI of 0.1 for one hour, followed by replacement of medium with
368 DMEM supplemented with 0.2 mg/mL TPCK-trypsin. Medium was replaced with fresh
369 0.2 mg/ml TPCK-trypsin containing DMEM each day until infection reached 100% CPE,
370 at which point medium was exchanged for DMEM lacking TPCK-trypsin. Cells were
371 incubated for additional 24 h to allow protein production. Supernatants were centrifuged
372 at 360 *g* for 5 min, then filtered with 0.1 μ m filter (Corning[®] 500 mL Vacuum
373 Filter/Storage Bottle System, 0.1 μ m Pore) to remove virions and debris. Supernatant
374 including RBD-Fc were applied to Protein G Sepharose (Millipore Sigma, #GE17-0618-
375 01) containing column (5ml Polypropylene Columns ;ThermoFisher, #29922), followed
376 by wash and elution.

377

378 **Human Subjects Research.**

379 Human subjects research was conducted following the Declaration of Helsinki and
380 related institutional and local regulations. Studies and serum collection relating to the
381 Sputnik vaccine at ANLIS Dr. Carlos G. Malbrán (National Administration Laboratories
382 and Health Institutes - Carlos G. Malbrán, Argentina) were approved by the Research
383 Ethics Committee of its Unidad Operativa Centro de Contención Biológica (UOCCB) on
384 9 Feb 2021.

385 **Authors contributions**

386 S.I., C.P., B.H.L., J.P.K, conceived of and supervised the study. C.P., A.E.V. and A.E.
387 supervised, collected, analyzed, and provided materials relevant to this study. S.I.
388 generated VSV-CoV-2 S plasmid and rescued viruses. S.I., G.H., S.K., and M.N.A.S.
389 were involved in the generation of S mutant viruses. S.I, L.B., M.N.A.S., K.Y.O.
390 conducted neutralization assays. S.I. and C.T.H. developed the Sendai virus protein
391 expressing system and purified RBD-Fc protein. S.I., B.H.L., and J.P.K. wrote the paper
392 with input from C.P. and all co-authors.

393

394 **Acknowledgements**

395 We gratefully acknowledge all submitting authors and collecting authors on whose work
396 this research is based, and to all researchers, clinicians, and public health authorities
397 who make SARS-CoV-2 sequence data available in a timely manner via the GISAID
398 initiative^{57,58}.

399

400 **Funding information**

401 We acknowledge the following finding. K.Y.O. was supported by Viral-Host
402 Pathogenesis Training Grant T32 AI07647 and additionally by a NRSA F31 AI154739.
403 S.I. and C.-T.H. were supported by postdoctoral fellowships from CHOT-SG (Fukuoka
404 University, Japan) and the Ministry of Science and Technology (MOST, Taiwan),
405 respectively. B.L. acknowledges flexible funding support from NIH grants AI123449 and
406 AI138921; a grant from the Department of Microbiology, Icahn School of Medicine at
407 Mount Sinai; and the Ward-Coleman estate, which endowed the Ward-Coleman Chairs
408 at the ISMMS. J.P.K. was supported by a COVID-19 Fast Grants award from Emergent
409 Ventures, an initiative of the Mercatus Center at George Mason University, and by an
410 intramural grant and other funding from the Office of the Vice Chancellor for Research
411 at LSU Health Sciences Center Shreveport (J.P.K., M.N.A.S.). Processing costs
412 recovered from multiple users of our standardized SARS-CoV-2 VSV pseudotyped
413 particles provided additional support (BL). Work at ANLIS-MALBRAN (A.E.V., A.E.,
414 C.P.) was supported by the Ministry of Health (Ministerio de Salud), Argentina.

415 **Table 1. Cohort characteristics of Sputnik vaccine recipients from ANLIS MALBRÁN**
 416 **(Buenos Aires, República Argentina).**

417

Sera ID	1 st DOSE	2 nd DOSE	Vaccine Status	SEX	AGE
SP001	Late Dec/2020	Mid Jan/2021	(+)	M	45-50
SP002	Late Dec/2020	Mid Jan/2021	(+)	M	40-45
SP003	Late Dec/2020	Mid Jan/2021	(+)	M	55-60
SP004	Late Dec/2020	Mid Jan/2021	(+)	M	50-55
SP005	Late Dec/2020	Mid Jan/2021	(+)	M	35-40
SP006	Late Dec/2020	Mid Jan/2021	(+)	F	35-40
SP007	Late Dec/2020	Mid Jan/2021	(+)	F	20-25
SP008	Late Dec/2020	Early Feb/2021	(+)	M	35-40
SP009	Late Dec/2020	Early Feb/2021	(+)	F	30-35
SP010	Late Dec/2020	Mid Jan/2021	(+)	M	30-35
SP011	Late Dec/2020	Mid Jan/2021	(+)	M	40-45
SP012	Late Dec/2020	Mid Jan/2021	(+)	M	25-30
				Median Age	39.5
				Range	25-56
SP013	N.A.	N.A.	(-)	F	45-50

SP014	N.A.	N.A.	(-)	F	50-55
SP015	N.A.	N.A.	(-)	M	40-45

418

N.A., Not Applicable

SUPPLEMENTAL TABLE 1. Acknowledgement of S: E484K viruses from South America shared on GISAID.

SUPPLEMENTAL TABLE 2. Acknowledgement of B.1.1.7 and B.1.351 viruses used for selection of S variants evaluated in this study.

REFERENCES

1. Huang, C. *et al.* Clinical features of patients infected with 2019 novel coronavirus in Wuhan, China. *Lancet* **395**, 497–506 (2020).
2. COVID-19 Map - Johns Hopkins Coronavirus Resource Center.
<https://coronavirus.jhu.edu/map.html>.
3. Cobey, S., Larremore, D. B., Grad, Y. H. & Lipsitch, M. Concerns about SARS-CoV-2 evolution should not hold back efforts to expand vaccination. *Nat. Rev. Immunol.* (2021) doi:10.1038/s41577-021-00544-9.
4. Wibmer, C. K. *et al.* SARS-CoV-2 501Y.V2 escapes neutralization by South African COVID-19 donor plasma. *Nat. Med.* (2021) doi:10.1038/s41591-021-01285-x.
5. Zhou, D. *et al.* Evidence of escape of SARS-CoV-2 variant B.1.351 from natural and vaccine-induced sera. *Cell* (2021) doi:10.1016/j.cell.2021.02.037.
6. Wang, P. *et al.* Increased Resistance of SARS-CoV-2 Variant P. 1 to Antibody Neutralization. *BioRxiv* (2021).
7. Liu, Y. *et al.* Neutralizing Activity of BNT162b2-Elicited Serum. *N. Engl. J. Med.* (2021) doi:10.1056/NEJMc2102017.
8. Garcia-Beltran, W. F. *et al.* Multiple SARS-CoV-2 variants escape neutralization by vaccine-induced humoral immunity. *Cell* (2021) doi:10.1016/j.cell.2021.03.013.
9. Boni, M. F. *et al.* Evolutionary origins of the SARS-CoV-2 sarbecovirus lineage responsible for the COVID-19 pandemic. *Nat Microbiol* **382**, 1199 (2020).
10. Logunov, D. Y. *et al.* Safety and efficacy of an rAd26 and rAd5 vector-based heterologous prime-boost COVID-19 vaccine: an interim analysis of a randomised controlled phase 3 trial in Russia. *Lancet* **397**, 671–681 (2021).

11. Baden, L. R. *et al.* Efficacy and safety of the mRNA-1273 SARS-CoV-2 vaccine. *N. Engl. J. Med.* **384**, 403–416 (2021).
12. Polack, F. P. *et al.* Safety and Efficacy of the BNT162b2 mRNA Covid-19 Vaccine. *N. Engl. J. Med.* **383**, 2603–2615 (2020).
13. Zhang, Y. *et al.* Safety, tolerability, and immunogenicity of an inactivated SARS-CoV-2 vaccine in healthy adults aged 18–59 years: a randomised, double-blind, placebo-controlled, phase 1/2 clinical trial. *Lancet Infect. Dis.* (2020).
14. Sadoff, J. *et al.* Interim Results of a Phase 1–2a Trial of Ad26.COV2.S Covid-19 Vaccine. *N. Engl. J. Med.* (2021) doi:10.1056/NEJMoa2034201.
15. Folegatti, P. M. *et al.* Safety and immunogenicity of the ChAdOx1 nCoV-19 vaccine against SARS-CoV-2: a preliminary report of a phase 1/2, single-blind, randomised controlled trial. *Lancet* **396**, 467–478 (2020).
16. Addetia, A. *et al.* Neutralizing Antibodies Correlate with Protection from SARS-CoV-2 in Humans during a Fishery Vessel Outbreak with a High Attack Rate. *J. Clin. Microbiol.* **58**, (2020).
17. Khoury, D. S. *et al.* What level of neutralising antibody protects from COVID-19? *bioRxiv* (2021) doi:10.1101/2021.03.09.21252641.
18. Andrew Rambaut, Nick Loman, Oliver Pybus, Wendy Barclay, Jeff Barrett, Alesandro Carabelli, Tom Connor, Tom Peacock, David L Robertson, Erik Volz, COVID-19 Genomics Consortium UK (CoG-UK). Preliminary genomic characterisation of an emergent SARS-CoV-2 lineage in the UK defined by a novel set of spike mutations. *Virological.org* <https://virological.org/t/preliminary-genomic-characterisation-of-an-emergent-sars-cov-2-lineage-in-the-uk-defined-by-a-novel->

- set-of-spike-mutations/563 (2020).
19. Choi, B. *et al.* Persistence and Evolution of SARS-CoV-2 in an Immunocompromised Host. *N. Engl. J. Med.* **383**, 2291–2293 (2020).
 20. Davies, N. G. *et al.* Estimated transmissibility and impact of SARS-CoV-2 lineage B.1.1.7 in England. *Science* (2021) doi:10.1126/science.abg3055.
 21. Davies, N. G. *et al.* Increased mortality in community-tested cases of SARS-CoV-2 lineage B.1.1.7. *Nature* (2021) doi:10.1038/s41586-021-03426-1.
 22. Grint, D. J. *et al.* Case fatality risk of the SARS-CoV-2 variant of concern B.1.1.7 in England. *bioRxiv* (2021) doi:10.1101/2021.03.04.21252528.
 23. Tegally, H. *et al.* Emergence and rapid spread of a new severe acute respiratory syndrome-related coronavirus 2 (SARS-CoV-2) lineage with multiple spike mutations in South Africa. *bioRxiv* (2020) doi:10.1101/2020.12.21.20248640.
 24. Naveca, F. *et al.* SARS-CoV-2 reinfection by the new Variant of Concern (VOC) P.1 in Amazonas, Brazil. *virological.org*. Preprint available at: <https://virological.org/t/sars-cov-2-reinfection-by-the-new-variant-of-concern-voc-p-1-in-amazonas-brazil/596> (2021).
 25. Dejnirattisai, W. *et al.* Antibody evasion by the Brazilian P.1 strain of SARS-CoV-2. *Cold Spring Harbor Laboratory* 2021.03.12.435194 (2021) doi:10.1101/2021.03.12.435194.
 26. Weisblum, Y. *et al.* Escape from neutralizing antibodies by SARS-CoV-2 spike protein variants. *Elife* **9**, (2020).
 27. Liu, Z. *et al.* Identification of SARS-CoV-2 spike mutations that attenuate monoclonal and serum antibody neutralization. *Cell Host Microbe* **0**, (2021).

28. Greaney, A. J. *et al.* Comprehensive mapping of mutations in the SARS-CoV-2 receptor-binding domain that affect recognition by polyclonal human plasma antibodies. *Cell Host Microbe* **29**, 463–476.e6 (2021).
29. West, A. P., Barnes, C. O., Yang, Z. & Bjorkman, P. J. SARS-CoV-2 lineage B.1.526 emerging in the New York region detected by software utility created to query the spike mutational landscape. *Cold Spring Harbor Laboratory* 2021.02.14.431043 (2021) doi:10.1101/2021.02.14.431043.
30. Annavajhala, M. K. *et al.* A novel SARS-CoV-2 variant of concern, B.1.526, identified in New York. *bioRxiv* (2021) doi:10.1101/2021.02.23.21252259.
31. Voloch, C. M. *et al.* Genomic characterization of a novel SARS-CoV-2 lineage from Rio de Janeiro, Brazil. *J. Virol.* (2021) doi:10.1128/JVI.00119-21.
32. Madhi, S. A. *et al.* Efficacy of the ChAdOx1 nCoV-19 Covid-19 Vaccine against the B.1.351 Variant. *N. Engl. J. Med.* (2021) doi:10.1056/NEJMoa2102214.
33. Logunov, D. Y. *et al.* Safety and immunogenicity of an rAd26 and rAd5 vector-based heterologous prime-boost COVID-19 vaccine in two formulations: two open, non-randomised phase 1/2 studies from Russia. *Lancet* **396**, 887–897 (2020).
34. Dieterle, M. E. *et al.* A Replication-Competent Vesicular Stomatitis Virus for Studies of SARS-CoV-2 Spike-Mediated Cell Entry and Its Inhibition. *Cell Host Microbe* **28**, 486–496.e6 (2020).
35. Li, H. *et al.* Establishment of replication-competent vesicular stomatitis virus-based recombinant viruses suitable for SARS-CoV-2 entry and neutralization assays. *Emerg. Microbes Infect.* **9**, 2269–2277 (2020).
36. Case, J. B. *et al.* Replication-Competent Vesicular Stomatitis Virus Vaccine Vector

- Protects against SARS-CoV-2-Mediated Pathogenesis in Mice. *Cell Host Microbe* **28**, 465–474.e4 (2020).
37. Baum, A. *et al.* Antibody cocktail to SARS-CoV-2 spike protein prevents rapid mutational escape seen with individual antibodies. *Science* **369**, 1014–1018 (2020).
 38. Yahalom-Ronen, Y. *et al.* A single dose of recombinant VSV- Δ G-spike vaccine provides protection against SARS-CoV-2 challenge. *Nat. Commun.* **11**, 6402 (2020).
 39. Greaney, A. J. *et al.* Complete Mapping of Mutations to the SARS-CoV-2 Spike Receptor-Binding Domain that Escape Antibody Recognition. *Cell Host Microbe* **29**, 44–57.e9 (2021).
 40. Oguntuyo, K. Y. *et al.* Quantifying absolute neutralization titers against SARS-CoV-2 by a standardized virus neutralization assay allows for cross-cohort comparisons of COVID-19 sera. *MBio* **12**, (2021).
 41. Webb, N. E., Montefiori, D. C. & Lee, B. Dose–response curve slope helps predict therapeutic potency and breadth of HIV broadly neutralizing antibodies. *Nat. Commun.* **6**, 1–10 (2015).
 42. Bos, R. *et al.* Ad26 vector-based COVID-19 vaccine encoding a prefusion-stabilized SARS-CoV-2 Spike immunogen induces potent humoral and cellular immune responses. *NPJ Vaccines* **5**, 91 (2020).
 43. Walsh, E. E. *et al.* Safety and Immunogenicity of Two RNA-Based Covid-19 Vaccine Candidates. *N. Engl. J. Med.* **383**, 2439–2450 (2020).
 44. Corbett, K. S. *et al.* SARS-CoV-2 mRNA vaccine design enabled by prototype pathogen preparedness. *Nature* **586**, 567–571 (2020).

45. Wrapp, D. *et al.* Cryo-EM structure of the 2019-nCoV spike in the prefusion conformation. *Science* **367**, 1260–1263 (2020).
46. Pallesen, J. *et al.* Immunogenicity and structures of a rationally designed prefusion MERS-CoV spike antigen. *Proc. Natl. Acad. Sci. U. S. A.* **114**, E7348–E7357 (2017).
47. Cele, S. *et al.* Escape of SARS-CoV-2 501Y. V2 from neutralization by convalescent plasma. *medRxiv* (2021).
48. Hoffmann, M. *et al.* SARS-CoV-2 variants B.1.351 and P.1 escape from neutralizing antibodies. *Cell* (2021) doi:10.1016/j.cell.2021.03.036.
49. Muik, A. *et al.* Neutralization of SARS-CoV-2 lineage B.1.1.7 pseudovirus by BNT162b2 vaccine-elicited human sera. *Science* **371**, 1152–1153 (2021).
50. Shen, X. *et al.* SARS-CoV-2 variant B.1.1.7 is susceptible to neutralizing antibodies elicited by ancestral spike vaccines. *Cell Host Microbe* (2021) doi:10.1016/j.chom.2021.03.002.
51. Abdool Karim, S. S. & de Oliveira, T. New SARS-CoV-2 Variants — Clinical, Public Health, and Vaccine Implications. *N. Engl. J. Med.* (2021) doi:10.1056/NEJMc2100362.
52. Buchholz, U. J., Finke, S. & Conzelmann, K. K. ... respiratory syncytial virus (BRSV) from cDNA: BRSV NS2 is not essential for virus replication in tissue culture, and the human RSV leader region acts as a functional *J. Virol.* (1999).
53. Ramsburg, E. *et al.* A vesicular stomatitis virus recombinant expressing granulocyte-macrophage colony-stimulating factor induces enhanced T-cell responses and is highly attenuated for replication in animals. *J. Virol.* **79**, 15043–

15053 (2005).

54. Case, J. B. *et al.* Neutralizing Antibody and Soluble ACE2 Inhibition of a Replication-Competent VSV-SARS-CoV-2 and a Clinical Isolate of SARS-CoV-2. *Cell Host Microbe* **28**, 475–485.e5 (2020).
55. Amanat, F. *et al.* A serological assay to detect SARS-CoV-2 seroconversion in humans. *Nat. Med.* (2020) doi:10.1038/s41591-020-0913-5.
56. Beaty, S. M. *et al.* Efficient and Robust Paramyxoviridae Reverse Genetics Systems. *mSphere* **2**, (2017).
57. Elbe, S. & Buckland-Merrett, G. Data, disease and diplomacy: GISAID's innovative contribution to global health. *Glob Chall* **1**, 33–46 (2017).
58. Shu, Y. & McCauley, J. GISAID: Global initiative on sharing all influenza data - from vision to reality. *Euro Surveill.* **22**, (2017).

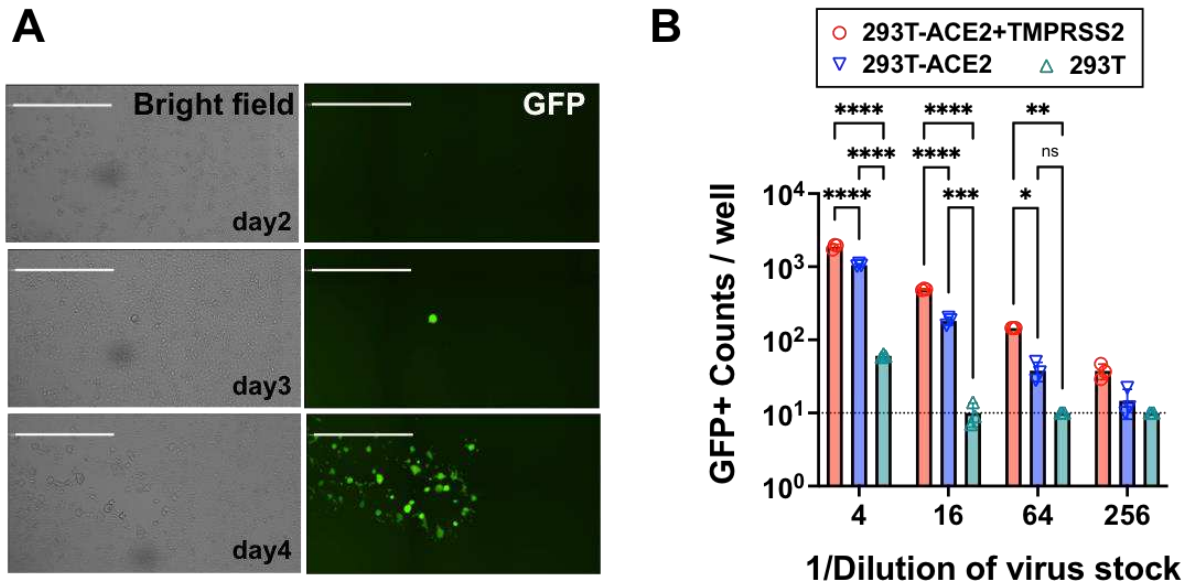


Figure 1. Generation of replication-competent VSV bearing SARS-CoV-2 spike (rcVSV-CoV2-S). (A) Representative images of *de novo* generation of rcVSV-CoV2-S, carrying an EGFP reporter, in transfected 293T-ACE2+TMPRSS2 (F8-2) cells as described in Extended Data Fig. S1. Single GFP+ cells detected at 2-3 days post-transfection (dpt) form a foci of syncytia by 4 dpt. Images are taken by Celigo imaging cytometer (Nexcelom) and are computational composites from the identical number of fields in each well. White bar is equal to 1 millimeter. (B) Entry efficiency of rcVSV-CoV2-S in parental 293T cells, 293T stably expressing ACE2 alone (293T-ACE2) or with TMPRSS2 (293T-ACE2+TMPRSS2). Serial dilutions of virus stocks amplified on Vero-TMPRSS2 cells were used to infect the indicated cell lines in 96-well plates in triplicates. GFP signal was detected and counted by a Celigo imaging cytometer (Nexcelom) 10 hours post-infection. Symbols are individual data points from triplicate infections at the indicated dilutions. Bars represent the average of 3 replicates with error bars indicating standard deviation. A two-way ANOVA was used to compare the differences between cell lines at any given dilution. Adjusted p values from Tukey's multiple comparisons test are given (ns; not significant, * $p < 0.05$, ** $p < 0.01$, *** $p < 0.001$, **** $p < 0.0001$).

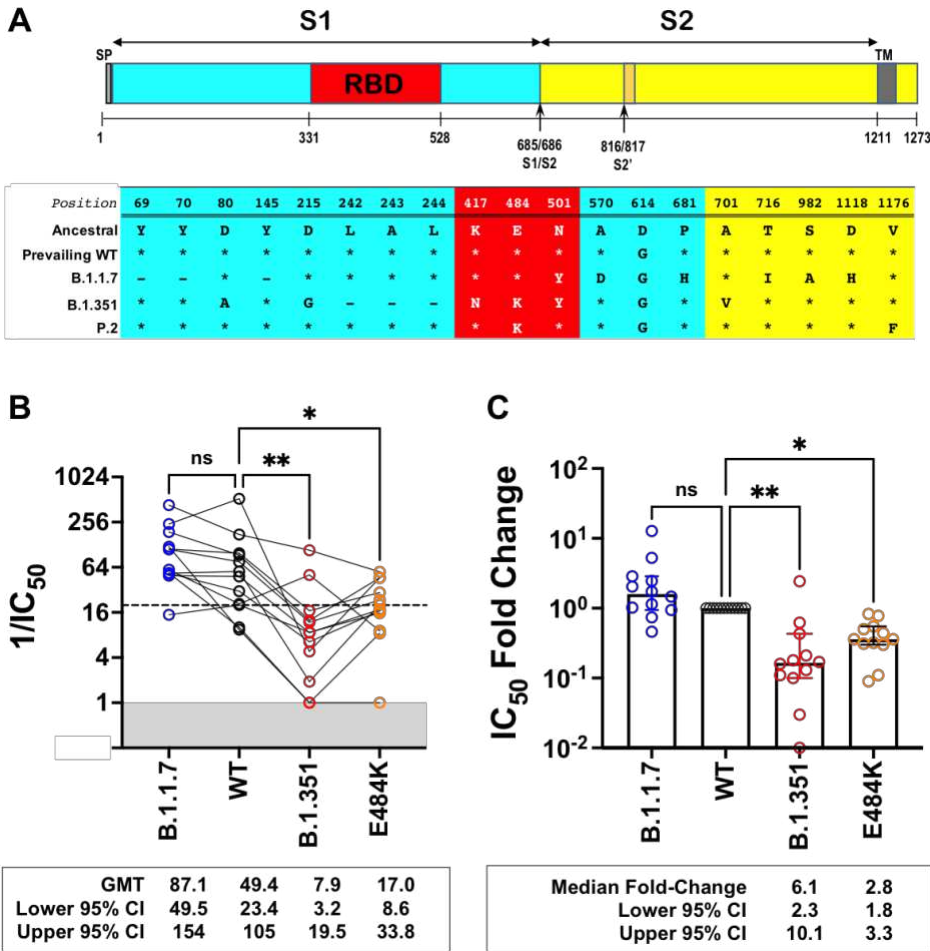


Figure 2. Neutralization activity of antibody responses elicited by the Sputnik V vaccine. (A) Schematic of the Spike substitutions that make up the variants being evaluated in this study. The amino acid positions and corresponding ‘Ancestral’ sequence of the Wuhan isolate is shown. The prevailing WT sequence now has a D614G substitution. All the variants and mutants have D614G. (B) Neutralization activity of individual serum samples against rcVSV-CoV2-S with the WT, variant (B.1.1.7 or B.1.351), or mutant E484K spike proteins. Neutralization is represented by the reciprocal 50% inhibitory dilution factor ($1/IC_{50}$). Sera samples with no appreciable neutralization against a given virus were assigned a defined $1/IC_{50}$ value of 1.0, as values ≤ 1 are not physiological (Grey shaded area). Dashed line indicates the lowest serum dilution tested ($1/IC_{50} = 20$). Geometric mean titers (GMT and 95% CI) for the neutralizing activity of all vaccine sera are indicated below each of the viral spike proteins examined. NS; not significant, *, $p < 0.05$, $p < 0.01$; ** are adjusted p values from non-parametric one-way ANOVA with Dunn’s multiple comparisons test. (C) For each serum sample, the fold-change in IC_{50} (reciprocal inhibitory dilution factor) against the indicated variant and mutant spike proteins relative to its IC_{50} against wild-type (WT) spike (set at 1) is plotted. Adjusted p values were calculated as in (B). Medians are represented by the bars and whiskers demarcate the 95% CI. Neutralization dose-response curves were performed in triplicates, and the mean values from each triplicate experiment are shown as the single data points for each sera sample.

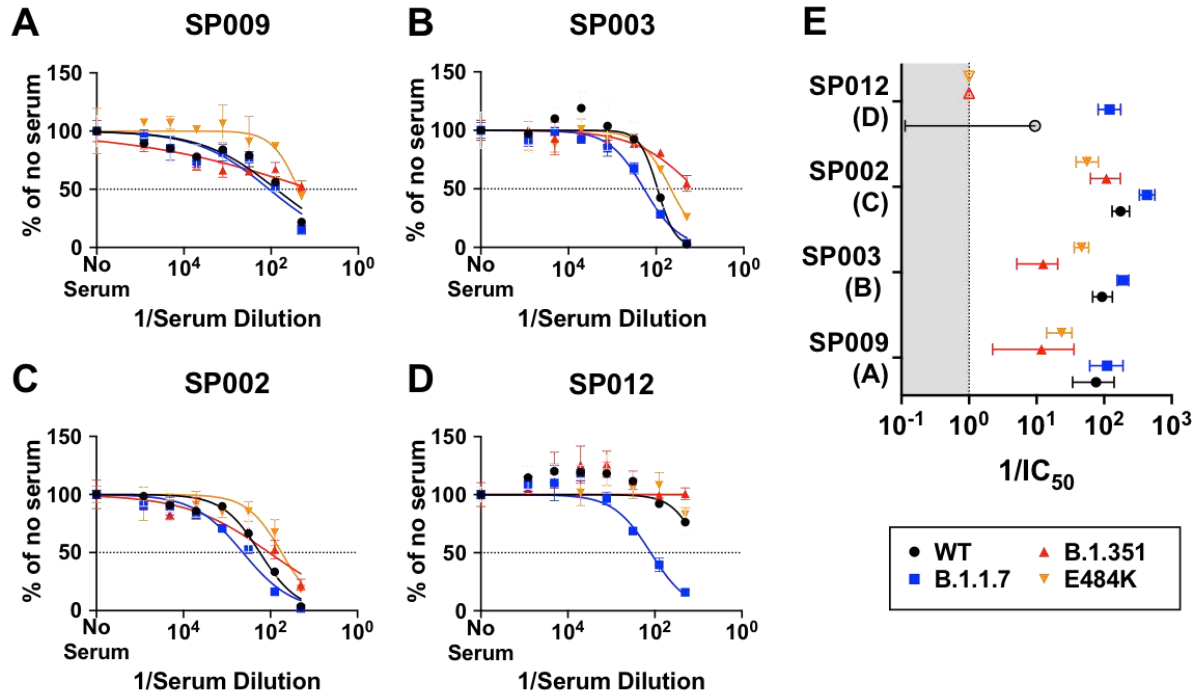


Figure 3. Dose response curves reveal distinct patterns of neutralizing antibody responses. Groups (A - D) represent distinct classes of virus neutralizing activity present in the sera samples analyzed. A representative member from each group is shown. Full neutralization curves for all sera tested against all viruses bearing the variant and mutant spike proteins are shown in supplementary Fig. S2. (E) graphs the virus neutralizing titers (VNT = $1/IC_{50}$) and 95% CI that can be extrapolated from the nonlinear regression curves. Different colored symbols represent the viruses indicated in the figure key. The open symbols in SP012 (Group D) represent assigned values of 1.0 (for B.1.351 and E484K) when no significant neutralization activity could be detected at the lowest serum dilution used (1:20) or ambiguous fits (for WT) due to very low neutralizing activity. The shaded area represents values that are not physiologically relevant.

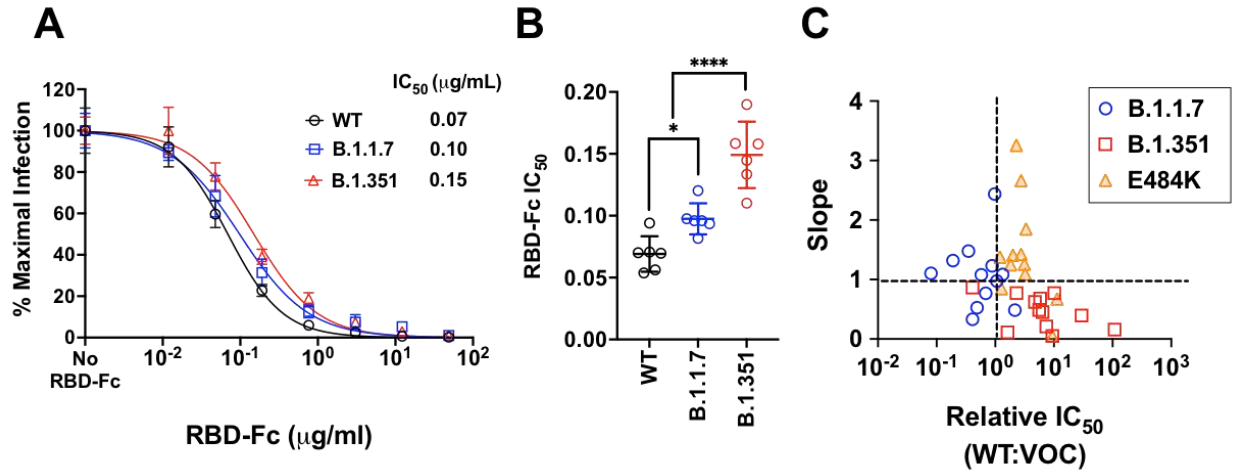
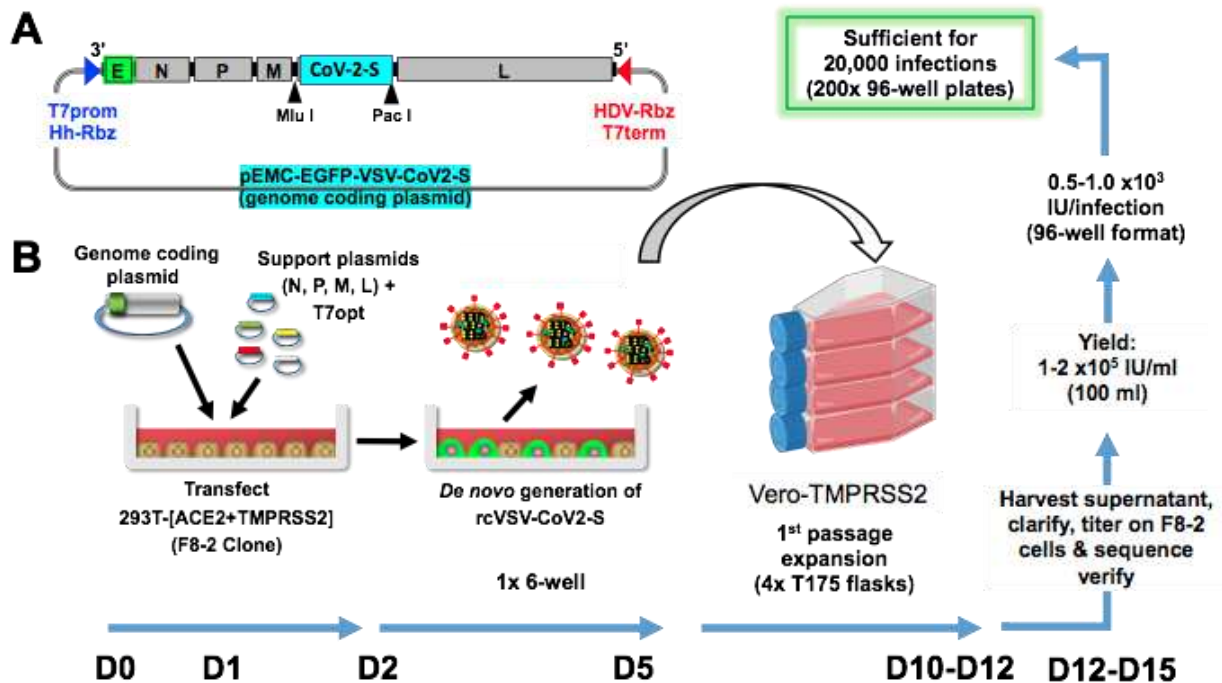
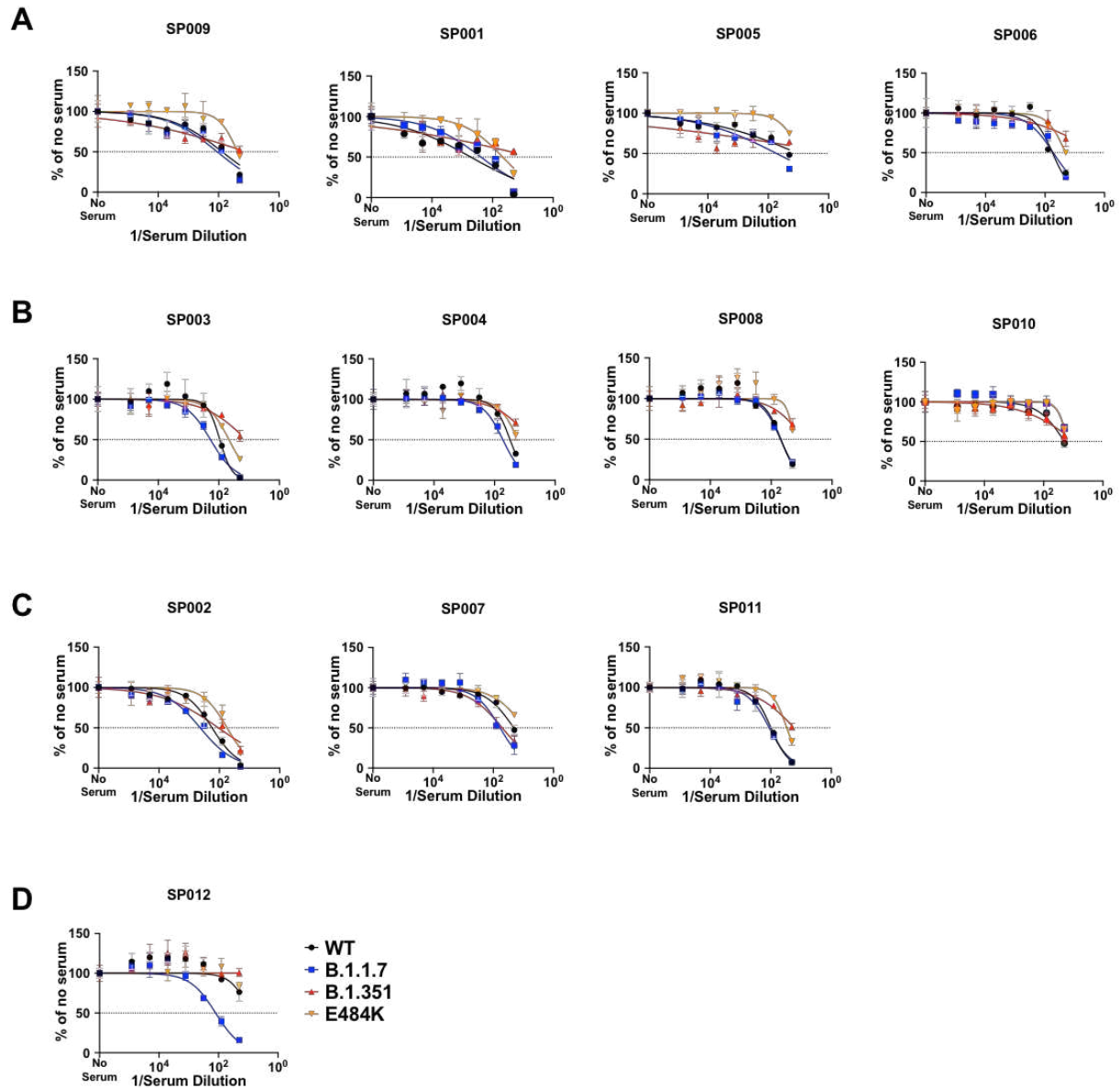


Figure 4. Competitive inhibition of rcVSV-CoV2-S entry by soluble RBD-Fc. (A)

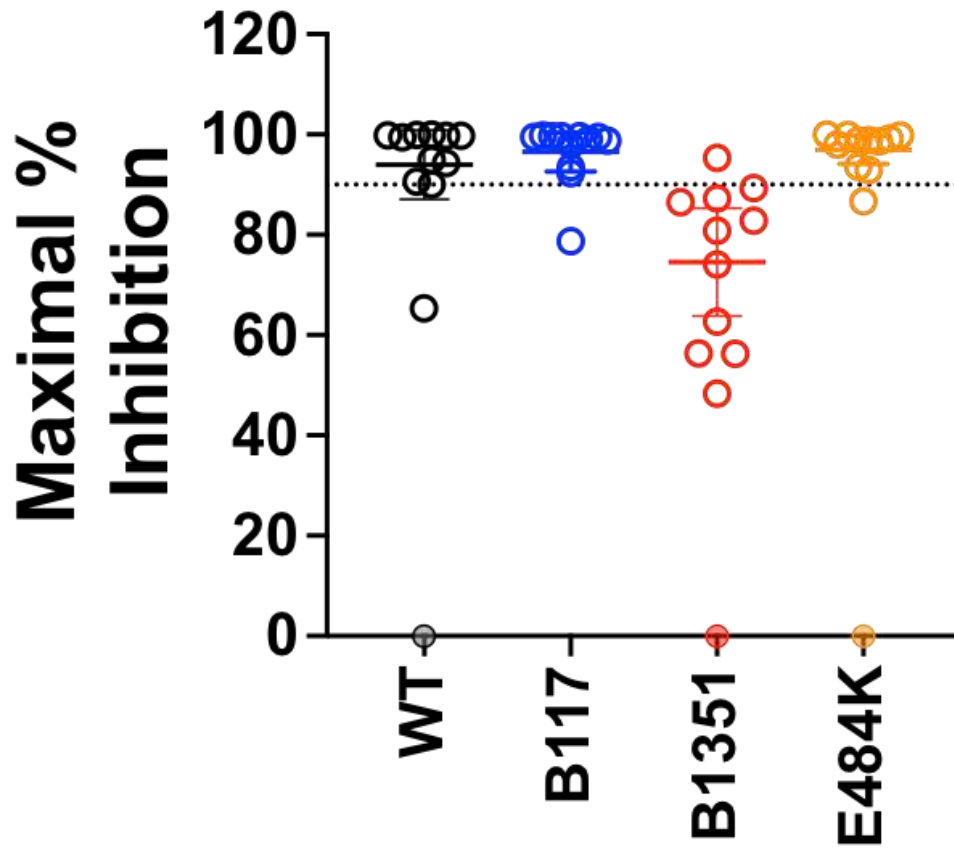
Recombinant RBD-Fc was serially titrated with the infection inoculum containing a fixed amount of rcVSV-CoV2-S bearing WT or the indicated VOC spike proteins. 10 hpi, GFP⁺ cells were quantified by the Celigo image cytometer. Data points are means of six independent replicates with error bars representing S.D. The number of GFP⁺ cells in the absence of any RBD-Fc was set to 100% and used to normalize the infection response in the presence of increasing amounts of RBD-Fc. Log[inhibitor] versus normalized response variable slope nonlinear regression curves were generated using GraphPad PRISM (v9.1.0). **(B)** The IC₅₀ values from each replicate dose response curve generated for a given virus were grouped. The mean (central bar) and SD (whiskers) for each group are indicated. Adjusted p values (*, p<0.05; ****, p<0.0001) from ordinary one-way ANOVA with Dunnett's multiple comparisons test are indicated. **(C)** Landscape of slope versus relative IC₅₀ values of all 12 Sputnik sera against the indicated VOC or mutant Spike. Relative IC₅₀ value is defined as the ratio of WT IC₅₀:VOC IC₅₀. Dashed lines indicate quadrants of high/low IC₅₀ and high/low slope.



Extended Data Figure S1. Robust and efficient generation of an EGFP-reporter replication-competent VSV bearing SARS-CoV-2 spike (rcVSV-CoV2-S). (A) Schematic of the rcVSV-CoV2-S genomic coding construct and the virus rescue procedure. The maximal T7 promoter (T7prom) followed by a hammer-head ribozyme (HhRbz) and the HDV ribozyme (HDVRbz) plus T7 terminator (T7term) are positioned at the 3' and 5' ends of the viral cDNA, respectively. An EGFP(E) transcriptional unit is placed at the 3' terminus to allow for high level transcription. SARS-CoV-2-S is cloned in place of VSV-G using the indicated restriction sites designed to facilitate easy exchange of spike variant or mutants. (B) For virus rescue, highly permissive 293T cells stably expressing human ACE2 and TMPRSS2 (293T-[ACE2+TMPRSS2], F8-2 clone) cells were transfected with the genome coding plasmid, helper plasmids encoding CMV-driven N, P, M, and L genes, and pCAGS encoding codon-optimized T7-RNA polymerase(T7opt). 48-72 hpi, transfected cells turn EGFP+ and start forming syncytia. Supernatant containing rcVSV-CoV2-S are then amplified in Vero-TMPRSS2 cells at the scale shown. The blue arrows at the bottom indicate the timeline for production of each sequence verified stock.



Extended Data Fig. S2. Sputnik vaccine elicits qualitatively different polyclonal responses against SARS-CoV-2 Spike. The full neutralization dose-response curves for all four classes of sera described in Fig. 3 are shown. Data points are mean of 3 independent replicates with error bars representing S.D. Infection (GFP+ cells) at each serum dilution was normalized to that obtained in the absence of any serum (set at 100%). Nonlinear regression of log [reciprocal serum dilution] versus normalized infection was performed using GraphPad PRISM (v9.0.1). Dotted lines represent 50% of maximal infection.



Extended Data Fig. S3. B.1.351 shows marked resistance to Sputnik vaccine sera neutralization.

Maximal Percent Inhibition (MPI) at full serum strength extrapolated from nonlinear regression of $\log(\text{inhibitor})$ versus normalized response, variable slope curve. Model used is from PRISM v9.0 where $Y = 100 / (1 + 10^{((\text{LogIC50} - X) * \text{HillSlope}))})$. Log IC50 and Hill slope values were obtained for each curve generated in Extended Data Fig. S2. For reciprocal serum dilution of 1 (10^0), $X = 0$. Shaded colored circles at $Y = 0$ for WT, B.1.351 and E484K represent data points from SP012 where no detectable neutralizing activity could be detected.

Figures

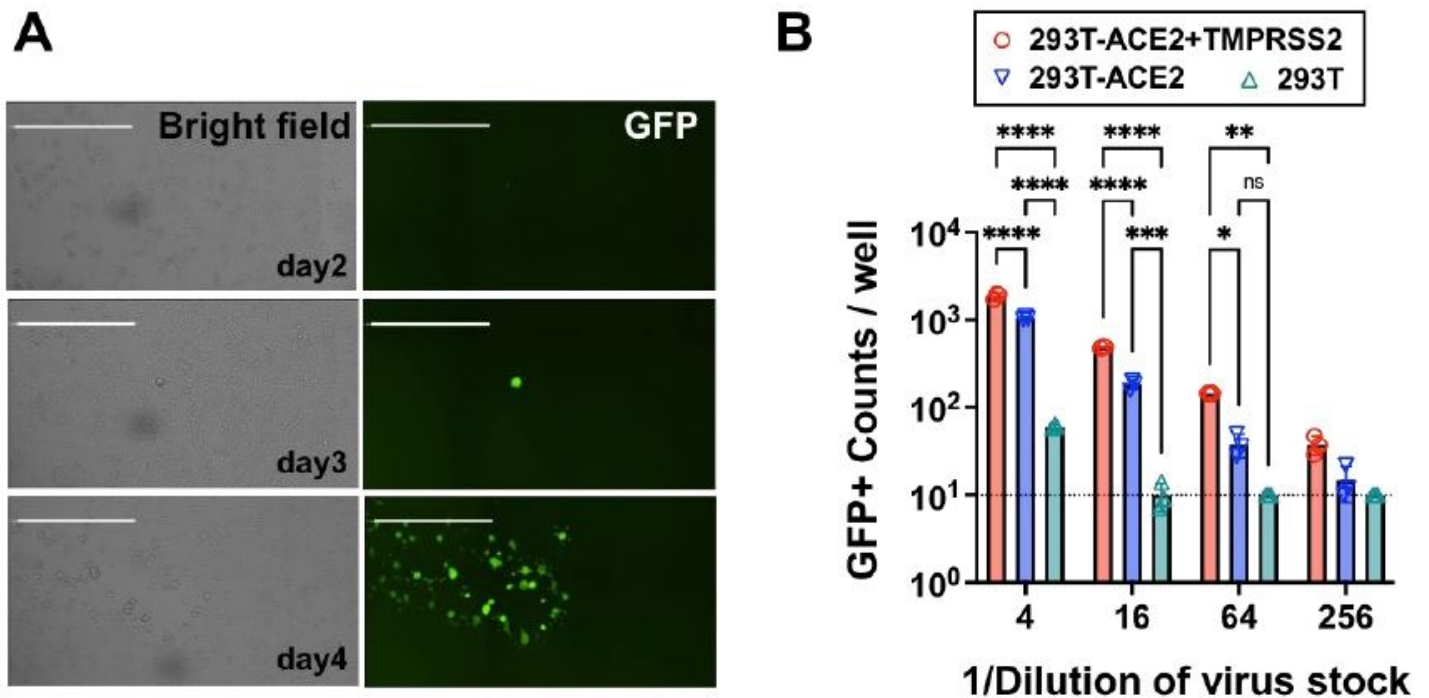


Figure 1

Generation of replication-competent VSV bearing SARS-CoV-2 spike (rcVSV-CoV2-S). (A) Representative images of de novo generation of rcVSV-CoV2-S, carrying an EGFP reporter, in transfected 293T-ACE2+TMPRSS2 (F8-2) cells as described in Extended Data Fig. S1. Single GFP+ cells detected at 2-3 days post-transfection (dpt) form a foci of syncytia by 4 dpt. Images are taken by Celigo imaging cytometer (Nexcelom) and are computational composites from the identical number of fields in each well. White bar is equal to 1 millimeter. (B) Entry efficiency of rcVSV-CoV2-S in parental 293T cells, 293T stably expressing ACE2 alone (293T-ACE2) or with TMPRSS2 (293T-ACE2+TMPRSS2). Serial dilutions of virus stocks amplified on Vero-TMPRSS2 cells were used to infect the indicated cell lines in 96-well plates in triplicates. GFP signal was detected and counted by a Celigo imaging cytometer (Nexcelom) 10 hours post-infection. Symbols are individual data points from triplicate infections at the indicated dilutions. Bars represent the average of 3 replicates with error bars indicating standard deviation. A two-way ANOVA was used to compare the differences between cell lines at any given dilution. Adjusted p values from Tukey's multiple comparisons test are given (ns; not significant, * $p < 0.05$, ** $p < 0.01$, *** $p < 0.001$, **** $p < 0.0001$).

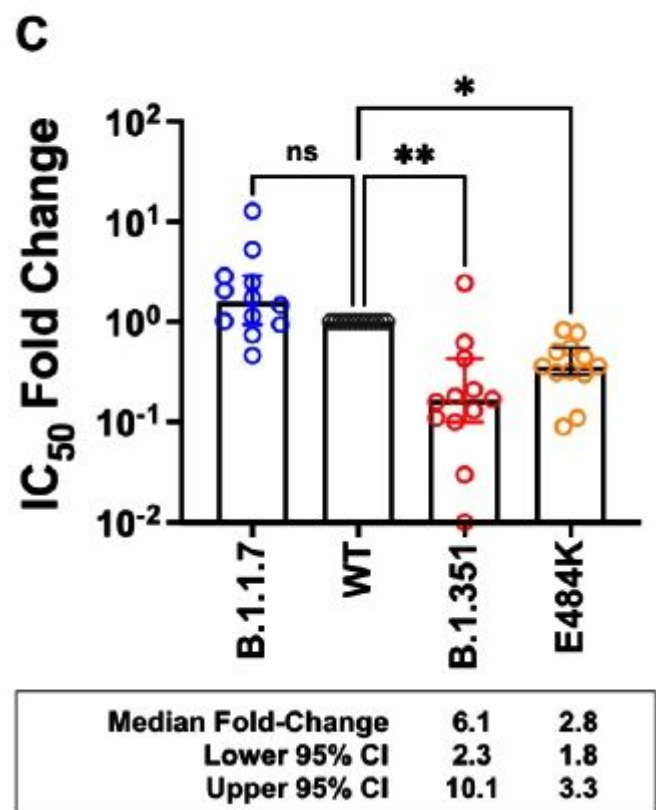
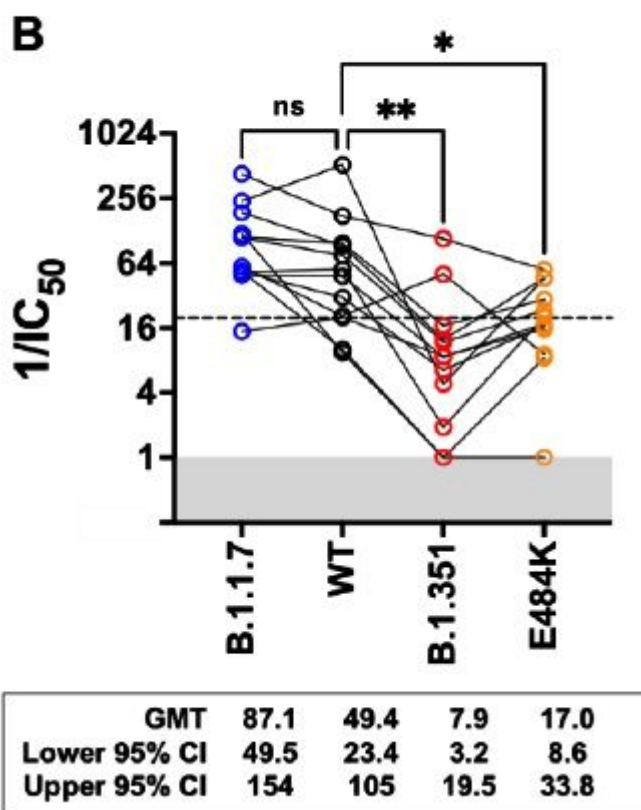
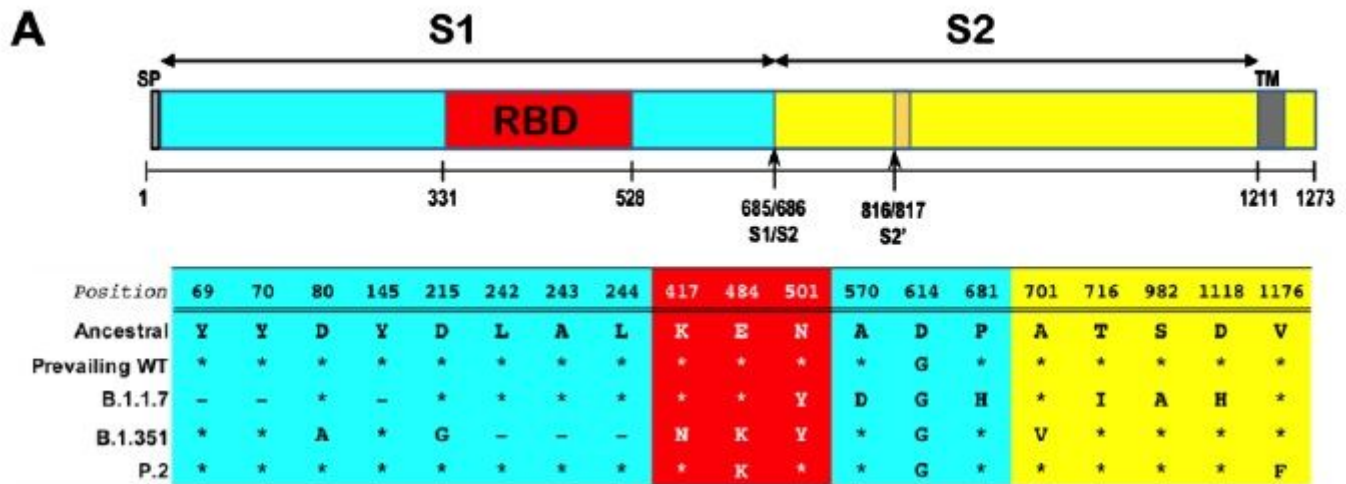


Figure 2

Neutralization activity of antibody responses elicited by the Sputnik V vaccine. (A) Schematic of the Spike substitutions that make up the variants being evaluated in this study. The amino acid positions and corresponding 'Ancestral' sequence of the Wuhan isolate is shown. The prevailing WT sequence now has a D614G substitution. All the variants and mutants have D614G. (B) Neutralization activity of individual serum samples against rcVSV-CoV2-S with the WT, variant (B.1.1.7 or B.1.351), or mutant E484K spike proteins. Neutralization is represented by the reciprocal 50% inhibitory dilution factor (1/IC₅₀). Sera samples with no appreciable neutralization against a given virus were assigned a defined 1/IC₅₀ value of 1.0, as values ≤1 are not physiological (Grey shaded area). Dashed line indicates the lowest serum

dilution tested ($1/IC_{50} = 20$). Geometric mean titers (GMT and 95% CI) for the neutralizing activity of all vaccine sera are indicated below each of the viral spike proteins examined. NS; not significant, *, $p < 0.05$, $p < 0.01$; ** are adjusted p values from non-parametric one-way ANOVA with Dunn's multiple comparisons test. (C) For each serum sample, the fold-change in IC_{50} (reciprocal inhibitory dilution factor) against the indicated variant and mutant spike proteins relative to its IC_{50} against wild-type (WT) spike (set at 1) is plotted. Adjusted p values were calculated as in (B). Medians are represented by the bars and whiskers demarcate the 95% CI. Neutralization dose-response curves were performed in triplicates, and the mean values from each triplicate experiment are shown as the single data points for each sera sample.

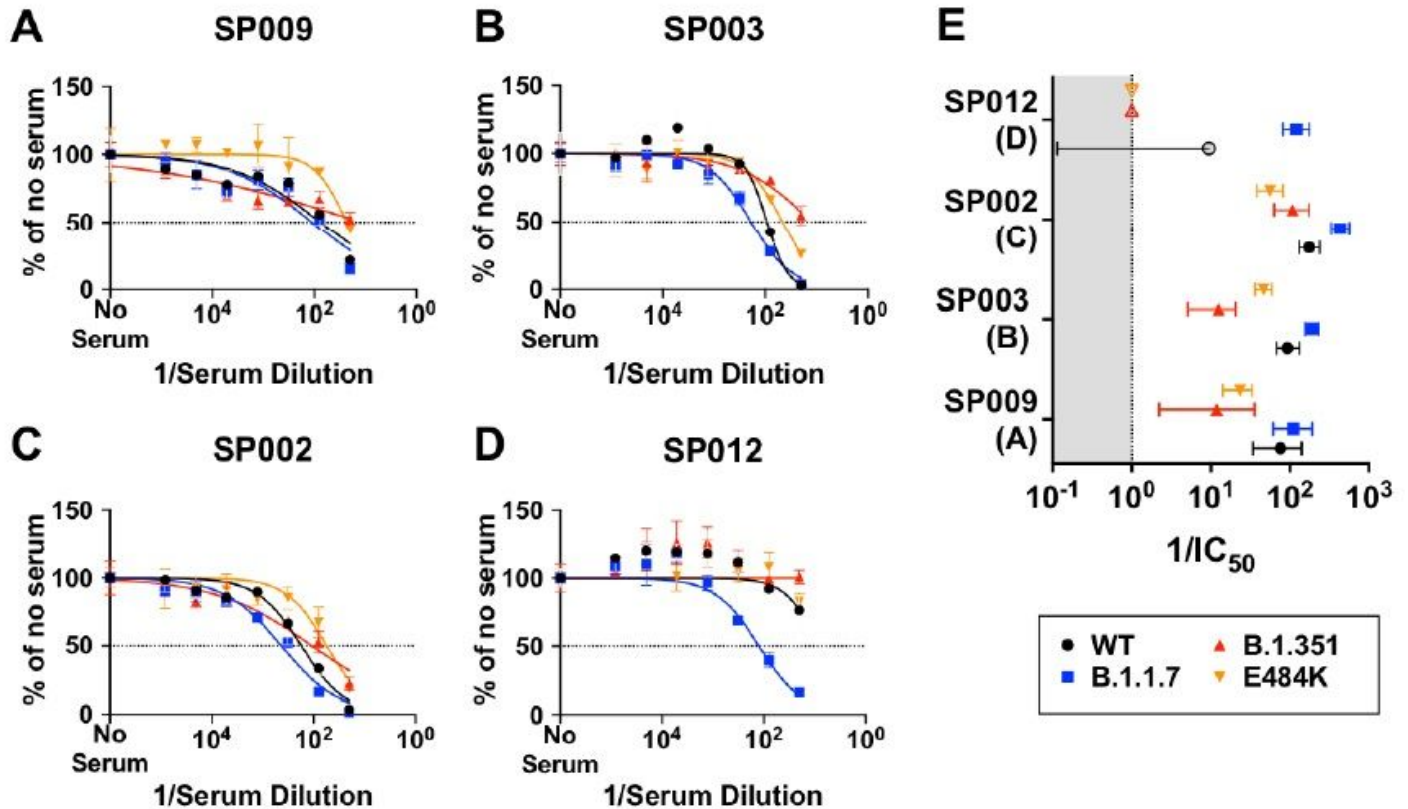


Figure 3

Dose response curves reveal distinct patterns of neutralizing antibody responses. Groups (A - D) represent distinct classes of virus neutralizing activity present in the sera samples analyzed. A representative member from each group is shown. Full neutralization curves for all sera tested against all viruses bearing the variant and mutant spike proteins are shown in supplementary Fig. S2. (E) graphs the virus neutralizing titers ($VNT = 1/IC_{50}$) and 95% CI that can be extrapolated from the nonlinear regression curves. Different colored symbols represent the viruses indicated in the figure key. The open symbols in SP012 (Group D) represent assigned values of 1.0 (for B.1.351 and E484K) when no significant neutralization activity could be detected at the lowest serum dilution used (1:20) or ambiguous fits (for WT) due to very low neutralizing activity. The shaded area represents values that are not physiologically relevant.

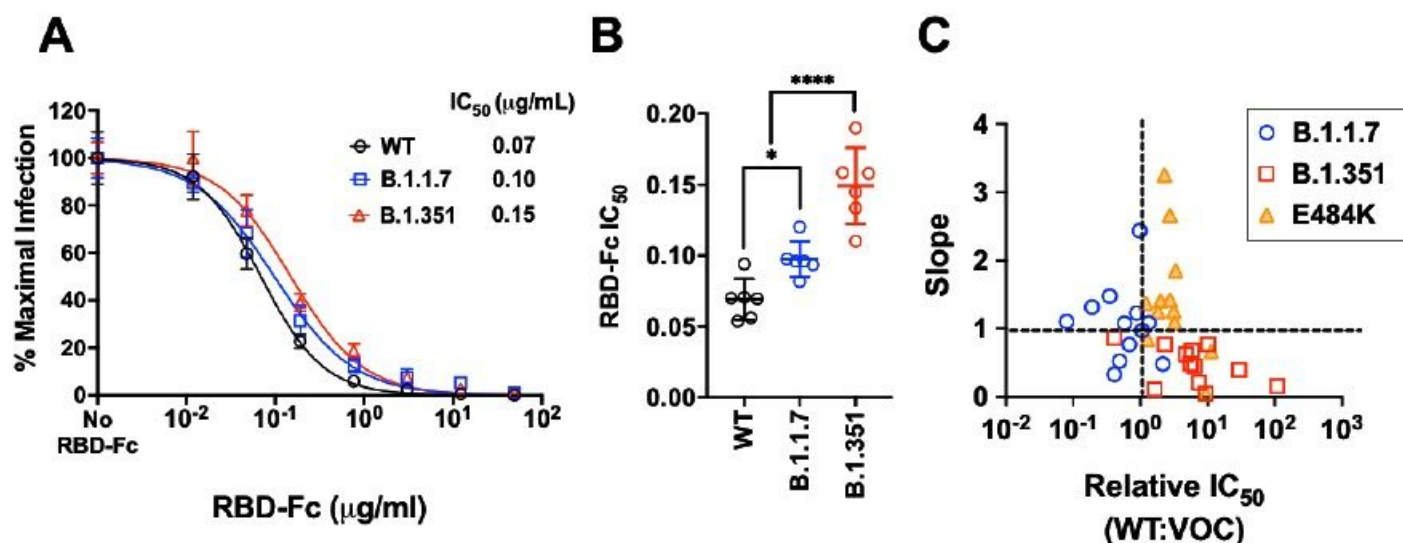


Figure 4

Competitive inhibition of rcVSV-CoV2-S entry by soluble RBD-Fc. (A) Recombinant RBD-Fc was serially titrated with the infection inoculum containing a fixed amount of rcVSV-CoV2-S bearing WT or the indicated VOC spike proteins. 10 hpi, GFP+ cells were quantified by the Celigo image cytometer. Data points are means of six independent replicates with error bars representing S.D. The number of GFP+ cells in the absence of any RBD-Fc was set to 100% and used to normalize the infection response in the presence of increasing amounts of RBD-Fc. Log[inhibitor] versus normalized response variable slope nonlinear regression curves were generated using GraphPad PRISM (v9.1.0). (B) The IC₅₀ values from each replicate dose response curve generated for a given virus were grouped. The mean (central bar) and SD (whiskers) for each group are indicated. Adjusted p values (*, p<0.05; ****, p<0.0001) from ordinary one-way ANOVA with Dunnett's multiple comparisons test are indicated. (C) Landscape of slope versus relative IC₅₀ values of all 12 Sputnik sera against the indicated VOC or mutant Spike. Relative IC₅₀ value is defined as the ratio of WT IC₅₀:VOC IC₅₀. Dashed lines indicate quadrants of high/low IC₅₀ and high/low slope.

Supplementary Files

This is a list of supplementary files associated with this preprint. Click to download.

- [SITable2B1351B117virussequencesused.pdf](#)
- [SITable1E484KvirusesSAmerica.pdf](#)
- [SITable1E484KvirusesSAmerica.pdf](#)
- [SITable2B1351B117virussequencesused.pdf](#)